BASALTIC SHERGOTTITE NORTHWEST AFRICA 856: DIFFERENTIATION OF A MARTIAN MAGMA. J. Ferdous[1], A.D. Brandon[1], A. H. Peslier[2] and Z. Pirotte[3]. [1]University of Houston, Houston TX 77204, USA, jferdous@uh.edu, [2]Jacobs, NASA-Johnson Space Center, Mail Code X13, Houston TX 77058, USA, [3]Dept. de Géologie, Université Libre de Bruxelles, 1050 Brussels, Belgium.

Introduction: Northwest Africa (NWA) 856 or Djel Ibone, is a basaltic shergottite discovered as a single stone of 320 g in South Morocco in April, 2001. This meteorite is fresh, i.e. shows minimal terrestrial weathering for a desert find [1]. No shergottite discovered in North Africa can be paired with NWA 856. The purpose of this study is to constrain its crystallization history using textural observations, crystallization sequence modeling and in-situ trace element analysis in order to understand differentiation in shergottite magmatic systems.

Analytical Techniques: A polished thick section (15 x 13 x 2 mm) was used for EDX-elemental mapping by scanning electron microscope (SEM). An electron microprobe (EMP) Camexa SX100 was used at NASA-Johnson Space Center to obtain in situ major element concentrations of each phase.

Major, minor and trace element abundances in minerals were measured using a Varian 810 inductively coupled plasma mass spectrometer connected to a CETAC LSX-213 laser ablation system (LA-ICP-MS) at the University of Houston. The sizes of the analyzed spots were 20-100 µm in diameter. The software GLITTER was used to calculate concentrations. Analyses were normalized to CaO contents obtained from EMP analyses. Basalt glass BHVO-2G (USGS standard) was used for calibration while BIR-1G (USGS standard) was used as an external standard to monitor accuracy and reproducibility.

Petrography: NWA 856 is a fine-grained, basaltic shergottite, typically Fe-rich and Al-poor compared to terrestrial basalts [1]. Although carbonate, from terrestrial weathering, is found in a few cracks, it is one of the least weathered among shergottites [1]. NWA 856 is similar to Shergotty and Zagami in texture, modal mineralogy, and bulk rock trace element abundances [1]. The major mineral modes of NWA856 are 45% pigeonite, 23% augite and 23% maskelynite (figure 1). The minor minerals present are ulvöspinel, ilmenite, merrillite, Cl-apatite, pyrrhotite, baddeleyite, amorphous K-feldspar and some other silica i.e. high-pressured stishovite [1], high-temperature cristobalite [2], quartz and glass.

Pigeonite and augite phenocrysts are elongated (up to ~6 mm), euhedral to subhedral grains, compositionally zoned and highly fractured. All pyroxenes have exsolution lamellae down to <1 µm wide [3]. The second dominant phase, maskelynite (plagioclase transformed to diaplectic glass by shock) is lath-shaped, irregularly branched, mostly devoid of fracture and interstitial to the pyroxenes. Impact melt pockets are present at the boundaries of pyroxenes and maskelynites that have various silica phases such as needle-like (~1 µm) high-pressured stishovite and silica glass, similar to Shergotty and NWA 480 [1]. Our findings are consistent with the analysis of Jambon et al. (2002). Only major exception we found is presence of exsolution in all pyroxenes [3].

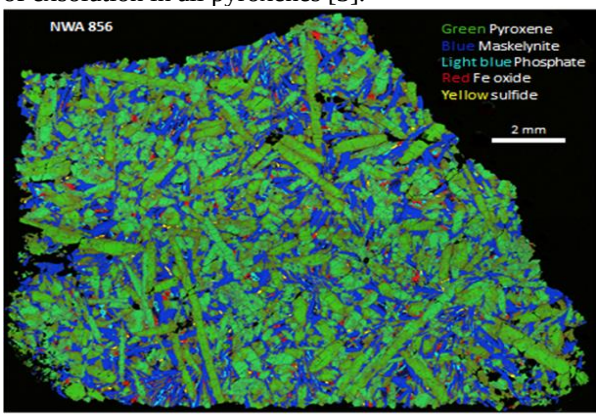

Figure 1: EDX-image of thick section of NWA 856.

Crystallization Sequence: The crystallization sequence of NWA 856 is derived from textural relationships and compared to results from a MELTS simulation [4] using NWA 856 bulk composition from [1] as initial composition. Ulvöspinel and pyroxenes crystallized first [5] in a slowly cooling basaltic melt, similar to basaltic shergottite NWA 5298 [6]. The Mg# decreases systematically from core to rim in both pigeonite (Mg# 0.42 to 0.2) and augite (Mg# 0.49 to 0.31) crystals which is a common feature of clinopyroxene in shergottites and terrestrial basalts [6]. In the MELTS simulation, MgO progressively decreases (Mg# 0.29 to 0.09) in the residual melt consistent with the earliest formation of Mg-rich pyroxene cores. Initial increases in the Ca-concentration is reflected in the early augite core crystallization before plagioclase starts crystallizing [7]. Based on progressive Fe, Al and Ca-decrease in the evolving melt, initiation of plagioclase formation occurs at the same time as the formation of the Fe-rich rims of the pyroxene. Close association of plagioclase with pyroxene rims supports this conclusion. Other minor mineral phases formed after the plagioclase formation. As with NWA 5298, ulvöspinel, clinopyroxene and plagioclase formation continued until the end of magma crystallization [6]. Olivine is present in the equilibrium MELTS simulation but is not ob-

served in NWA 856. MELTS simulation, result in the same crystallization sequences at 4 kbar (figure 2) and 5 kbar and those run under fractionation conditions are most consistent with our textural analysis [6].

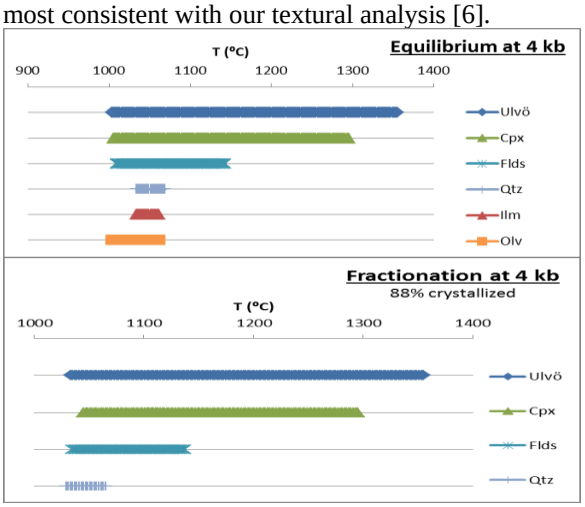

Figure 2: Crystallization sequence based on MELTS simulation of isobaric equilibrium and fractional crystallization.

In-situ Trace-element Concentrations: The pyroxenes have slightly LREE-depleted patterns, resembling REE patterns in clinopyroxenes in other shergottites [8]. The REE patterns are sub-parallel to each other with increasing concentrations from core to rim of pigeonite, to core to rim of augite (figure 3). The cores being more depleted in REE than the rims and compatible element (i.e. Cr and V) concentrations being higher in pyroxene cores than their rims is consistent with progressive crystallization in an evolving magma [9,10].

Two compositional types of maskelynite are present, a P-rich (P= 0.64%) and a P-poor (P= 0.046%) type. Both varieties have flat REE-patterns with positive Eu-anomalies (Figure 3). Unlike maskelynite in NWA 5298, HREE are not more depleted than the LREE [6,10]. The P-rich maskelynite has elevated REE-abundances and only a slightly positive Eu-anomaly consistent with phosphate assimilation during shock melting [9,10]. The P-poor maskelynite has lower REE abundances with highly positive Eu-anomalies, and may represent the original pre-shock plagioclase composition [9,10].

Clinopyroxenes do not show an increase in P from core to rim with the exception of the pigeonite rims. This indicates that the clinopyroxenes and in particular, their cores were not disturbed by shock or alteration and they did not react with phosphates in post-crystallization processes [6]. This confirms that the enrichment in REE from core to rim in the pigeonites may have resulted from progressive crystallization of the evolving magma.

Merrillite and Cl-apatite have the highest amounts of REE among all phases, similar to those found in other shergottites [8,9]. The flat REE pattern of the phosphates results in a flat bulk-rock REE pattern, characteristic of the enriched group of shergottites [11]. Their slightly negative Eu-anomalies indicate late stage formation after plagioclase crystallization. The absence of positive Ce-anomalies and lower contents of Cs, Ba and Sr in all phases when compared to other desert finds (DaG 476, Dhofar 019, Los Angeles, NWA 1068) indicate that NWA 856 is the least affected by terrestrial weathering and alteration [1,12,13].

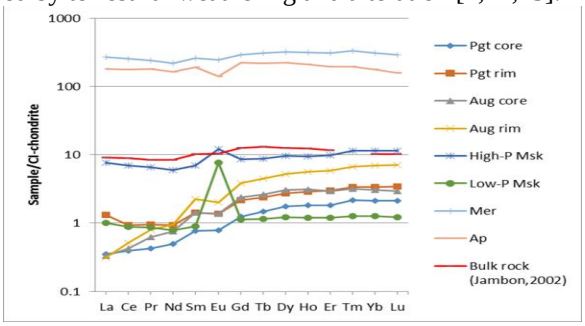

Figure 3: CI-chondrite normalized REE-patterns of zoned clinopyroxenes, plagioclases, phosphates and bulk composition in NWA 856.

Discussion and Conclusion: The results of petrography, EMP, LA-ICP-MS analyses and MELTS simulations are consistent with the findings of [1]. Pyroxene and spinel began to crystallize first. This was followed by a multistage crystallization sequence with plagioclase formation and final crystallization of phosphates and ilmenite. Pyroxene cores are not disturbed by alteration or shock but plagioclase was shocked into maskelynite with local incorporation of phosphates. NWA 856 closely resembles Shergotty and Zagami, but the lack of mesostasis, larger grain size, an abundance of impact melt pockets and minimal terrestrial weathering separate NWA 856 from any other basaltic shergottites.

References:

[1] Jambon et al. (2002), *MAPS, 37*, 1147-1164.
[2] Leroux and Cordier (2006), *MAPS, 41*, 913-923.
[3] Leroux et al. (2004), *MAPS, 39*, 711-722.
[4] Asimow and Ghiorso (1998), *AM, 83*, 1127-1131.
[5] Peslier et al. (2010), *GCA, 74*, 4543-4576.
[6] Hui et al. (2011), *MAPS, 46*, 1313-1328.
[7] Grove and Raudsepp (1978), *LPSC IX*, #585-599.
[8] Wadhwa et al. (1994), *GCA, 58*, 4213-4229.
[9] Basu Sarbadhikari et al. (2009), *GCA, 73*, 2190-2214.
[10] Shafer et al. (2010), *GCA, 74*, 7307-7328.
[11] Bridges and Warren (2006), *JGSL, 163*, 229-251.
[12] Brandon et al. (2004), *LPSC XXXV*, #1931.
[13] Barrat et al. (2002), *GCA, 66*, 3505-3518.